

Unusual Frequency Dispersion Effects of the Nonlinear Optical Response in Highly Conjugated (Polypyridyl)metal–(Porphinato)zinc(II) Chromophores

H. Tetsuo Uyeda,[†] Yuxia Zhao,[‡] Kurt Wostyn,[‡] Inge Asselberghs,[‡] Koen Clays,^{*,‡} André Persoons,^{*,‡} and Michael J. Therien^{*,†}

Contribution from the Department of Chemistry, University of Pennsylvania, Philadelphia, Pennsylvania 19104-6323 and Center for Research on Molecular Electronics and Photonics, University of Leuven, B-3001 Leuven, Belgium

Received May 6, 2002

Abstract: The syntheses and electrooptic properties of a new family of nonlinear optical chromophores are reported. These species feature an ethyne-elaborated, highly polarizable porphyrinic component and metal polypyridyl complexes that serve as integral donor and acceptor elements. Examples of this structural motif include ruthenium(II) [5-(4'-ethynyl-(2,2';6',2''-terpyridinyl))-10,20-bis(2',6'-bis(3,3-dimethyl-1-butyloxy)phenyl)porphinato]zinc(II)-(2,2';6',2''-terpyridine)²⁺ bis-hexafluorophosphate (Ru-PZn); osmium(II) [5-(4'-ethynyl-(2,2';6',2''-terpyridinyl))-10,20-bis(2',6'-bis(3,3-dimethyl-1-butyloxy)phenyl)porphinato]zinc(II)-(2,2';6',2''-terpyridine)²⁺ bis-hexafluorophosphate (Os-PZn); ruthenium(II) [5-(4'-ethynyl-(2,2';6',2''-terpyridinyl))-15-(4'-nitrophenyl)ethynyl-10,20-bis(2',6'-bis(3,3-dimethyl-1-butyloxy)phenyl)porphinato]zinc(II)-(2,2';6',2''-terpyridine)²⁺ bis-hexafluorophosphate (Ru-PZn-A); osmium(II) [5-(4'-ethynyl-(2,2';6',2''-terpyridinyl))-15-(4'-nitrophenyl)ethynyl-10,20-bis(2',6'-bis(3,3-dimethyl-1-butyloxy)phenyl)porphinato]zinc(II)-(2,2';6',2''-terpyridine)²⁺ bis-hexafluorophosphate (Os-PZn-A); and ruthenium(II) [5-(4'-ethynyl-(2,2';6',2''-terpyridinyl))osmium(II)-15-(4'-ethynyl-(2,2';6',2''-terpyridinyl))-10,20-bis(2',6'-bis(3,3-dimethyl-1-butyloxy)phenyl)porphinato]zinc(II)-bis(2,2';6',2''-terpyridine)⁴⁺ tetrakis-hexafluorophosphate (Ru-PZn-Os). The frequency dependence of the dynamic hyperpolarizability of these compounds was determined from hyperRayleigh light scattering (HRS) measurements carried out at fundamental incident irradiation wavelengths (λ_{inc}) of 800, 1064, and 1300 nm. These data show that (i) coupled oscillator photophysics and metal-mediated cross-coupling can be exploited to elaborate high β_0 supermolecules that exhibit significant excited-state electronic communication between their respective pigment building blocks; (ii) high-stability metal polypyridyl compounds constitute an attractive alternative to electron releasing dialkyl- and diarylamino groups, the most commonly used donor moieties in a wide range of established nonlinear optical dyes; (iii) this design strategy enables ready elaboration of chromophores having extraordinarily large dynamic hyperpolarizabilities (β_λ values) at telecommunication relevant wavelengths; and (iv) porphyrin B- and Q-state-derived static hyperpolarizabilities (β_0 values) can be designed to have the same or opposite sign in these species, thus providing a new means to regulate the magnitude of λ_{inc} -specific dynamic hyperpolarizabilities.

Introduction

Conventional chromophores for nonlinear optical (NLO) applications are based typically on design concepts that involve optimizing the electron releasing and electron withdrawing components, or conjugation length, of a particular dye platform.^{1–4}

We demonstrate as an alternative strategy that appropriate coupling of multiple charge transfer (CT) oscillators can give rise to supermolecular systems which feature substantial dynamic hyperpolarizabilities (β_λ values).

We report herein archetypal examples of such supermolecular NLO chromophores, describing their synthesis, electronic spectroscopy, potentiometric properties, and frequency-dependent hyperpolarizabilities determined via hyperRayleigh light scattering (HRS) measurements. These systems exploit an ethyne-elaborated, highly polarizable porphyrinic component and metal polypyridyl complexes that serve as integral donor (D) and acceptor (A) elements; examples of such structures are shown in Chart 1.

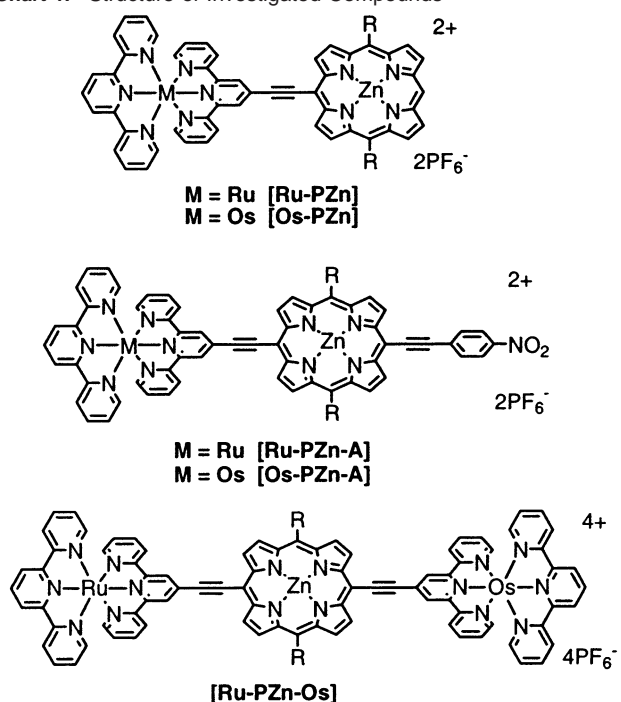
The rigid, cylindrically π -symmetric connectivity between the [porphinato]zinc(II) (PZn) and metal(II)polypyridyl units in

* To whom correspondence may be sent. E-mail: koen.clays@fys.kuleuven.ac.be; andre.persoons@fys.kuleuven.ac.be; therien@a.chem.upenn.edu.

[†] University of Pennsylvania.

[‡] University of Leuven.

- (1) Verbiest, T.; Houbrechts, S.; Kauranen, M.; Clays, K.; Persoons, A. *J. Mater. Chem.* **1997**, *7*, 2175–2189.
- (2) Marder, S. R.; Kippelen, B.; Jen, A. K. Y.; Peyghambarian, N. *Nature (London)* **1997**, *388*, 845–851.
- (3) Dalton, L. R.; Steier, W. H.; Robinson, B. H.; Zhang, C.; Ren, A.; Garner, S.; Chen, A.; Londergan, T.; Irwin, L.; Carlson, B.; Fifeild, L.; Phelan, G.; Kincaid, C.; Amend, J.; Jen, A. *J. Mater. Chem.* **1999**, *9*, 1905–1920.
- (4) Wolff, J. J.; Wortmann, R. *Adv. Phys. Org. Chem.* **1999**, *32*, 121–217.

Chart 1. Structure of Investigated Compounds

these systems aligns the CT transition dipoles of the chromophoric components in a head-to-tail arrangement and enforces exceptional excited-state interpigment electronic communication within the supermolecule. The electrooptic properties of these assemblies not only underscore the prominent role that coupled oscillator photophysics can play in the elaboration of chromophores with exceptional dynamic hyperpolarizabilities. They demonstrate also that such photophysics provides a powerful means to engineer frequency dispersion effects in the chromophoric NLO response that have, heretofore, been without precedent.

Experimental Section

Materials. All manipulations were carried out under nitrogen previously passed through an O₂ scrubbing tower (Schweizerhall R3-11 catalyst) and a drying tower (Linde 3-Å molecular sieves) unless otherwise stated. Air-sensitive solids were handled in a Braun 150-M glovebox. Standard Schlenk techniques were employed to manipulate air-sensitive solutions. All solvents utilized in this work were obtained from Fisher Scientific (HPLC Grade). Tetrahydrofuran (THF) was distilled from Na/benzophenone under N₂. Diethylamine and triethylamine were dried over KOH pellets and distilled under vacuum. All NMR solvents were used as received. Reagents 3,3-dimethyl-1-butanol, resorcinol, diethylazodicarboxylate (DEAD), triphenylphosphine (PPh₃), *n*-butyllithium, boron trifluoride etherate (BF₃·OEt₂), tetramethylethylenediamine (TMEDA), 1,2-dichloro-4,5-dicyanobenzoquinone (DDQ), 2,6-bis-pyridyl-4-(1H)-pyridone, phosphorus pentabromide (PBr₅), phosphorus oxybromide (POBr₃), potassium carbonate (K₂CO₃), potassium nitrate (KNO₃), potassium fluoride, *N*-ethylmorpholine, ammonium hexafluorophosphate (NH₄PF₆), sodium borohydride, trifluoroacetic acid, *N*-bromosuccinimide (NBS), zinc(II) acetate, TBAF (1 M in THF), methyl lithium (lithium bromide complex, 1.5 M, hexanes), 2,2',6',2''-terpyridine (tpy), RuCl₃, Na₂OsCl₆, trimethylsilylacetylene, triisopropylsilylacetylene, ZnCl₂ Pd₂dba₃, AsPh₃, Pd(PPh₃)₄, triisopropylamine, and copper(I) iodide were used as received (Aldrich or Strem). Compounds 2,2'-dipyrrylmethane,⁵ trimethylsilylethynyl zinc chloride,⁶ 4'-bromo-(2,2',6',2''-terpyridine)⁷⁻¹⁰ (Br-tpy), Ru(tpy)Cl₃,¹¹⁻¹⁵ and Os(tpy)Cl₃¹⁶⁻²⁰ were prepared by literature methods. Chemical shifts

for ¹H NMR spectra are relative to the solvent residual protium (CDCl₃, δ = 7.24 ppm; acetonitrile-*d*₃, δ = 1.93 ppm; pyridine-*d*₅, δ = 8.74 ppm). All *J* values are reported in Hertz. The number of attached protons is found in parentheses, following the chemical shift value. Chromatographic purification (silica gel 60, 230–400 mesh, EM Scientific) of all newly synthesized compounds was accomplished on the benchtop. High-resolution mass spectroscopic analyses were performed at the University of Pennsylvania Mass Spectrometry Center. Standard abbreviations for metal polypyridyl compounds and terpyridyls are used throughout the Experimental Section.

Instrumentation. Electronic spectra were recorded on an OLIS UV-vis/near-IR spectrophotometry system that is based on the optics of a Cary 14 spectrophotometer. Emission spectra were recorded on a SPEX Fluorolog luminescence spectrophotometer that utilized a T-channel configuration with a red sensitive R2658 Hamamatsu PMT and liquid nitrogen cooled InGaAs detector; these spectra were corrected using the spectral output of a calibrated light source supplied by the National Bureau of Standards. Cyclic voltammetric measurements were carried out on an EG&G Princeton Applied Research model 273A potentiostat/galvanostat. The electrochemical cell used for these experiments utilized a platinum disk working electrode, a platinum wire counter electrode, and a saturated calomel reference electrode (SCE). The reference electrode was separated from the bulk solution by a junction bridge filled with the corresponding solvent/supporting electrolyte solution. The ferrocene/ferrocenium redox couple was utilized as an internal potentiometric standard.

HyperRayleigh Light Scattering (HRS) Measurements. The experimental setup for the nanosecond hyperRayleigh scattering experiments at 1064 nm has been described in detail.²¹ Femtosecond HRS experiments were performed at 800 nm²² and at 1300 nm.²³ The chromophores were dissolved in dichloromethane and passed through 0.2-μm filters. Crystalviolet chloride (CV, 338 × 10⁻³⁰ esu in CH₃OH), *p*-nitroaniline (PNA, 21.6 × 10⁻³⁰ esu in CH₂Cl₂), and disperse red 1 (DRI, 54 × 10⁻³⁰ esu in CHCl₃) were utilized as reference chromophores at 800, 1064, and 1300 nm, respectively. For these external references in different solvents, standard local field correction factors were applied [(*n*_D² + 2)/3]³, where *n* is the refractive index of the solvent at the sodium D line]. Note that these experiments were performed at low chromophore concentrations [$< 3 \times 10^{-6} \text{ M}^{-1}$ (1064

- (5) Lin, V. S.-Y.; Iovine, P. M.; DiMugno, S. G.; Therien, M. J. *Inorg. Synth.* **2002**, *33*, 55–61.
- (6) Lin, V. S.-Y.; DiMugno, S. G.; Therien, M. J. *Science (Washington D. C.)* **1994**, *264*, 1105–1111.
- (7) Grossshenny, V.; Ziessel, R. *J. Organomet. Chem.* **1993**, *453*, C19–C22.
- (8) Grossshenny, V.; Romero, F. M.; Ziessel, R. *J. Org. Chem.* **1997**, *62*, 1491–1500.
- (9) Whittle, B.; Batten, S. R.; Jeffery, J. C.; Rees, L. H.; Ward, M. D. *J. Chem. Soc., Dalton Trans.* **1996**, 4249–4255.
- (10) Osawa, M.; Sonoki, H.; Hoshino, M.; Wakatsuki, Y. *Chem. Lett.* **1998**, 1081–1082.
- (11) Coe, B. J.; Thompson, D. W.; Culbertson, C. T.; Schoonover, J. R.; Meyer, T. J. *Inorg. Chem.* **1995**, *34*, 3385–3395.
- (12) Constable, E. C.; Ward, M. D. *J. Chem. Soc., Dalton Trans.* **1990**, 1405–1409.
- (13) Vogler, L. M.; Franco, C.; Jones, S. W.; Brewer, K. J. *Inorg. Chim. Acta* **1994**, *221*, 55–59.
- (14) Kober, E. M.; Marshall, J. L.; Dressick, W. J.; Sullivan, B. P.; Caspar, J. V.; Meyer, T. J. *Inorg. Chem.* **1985**, *24*, 2755–2763.
- (15) Adcock, P. A.; Keene, F. R.; Smythe, R. S.; Snow, M. R. *Inorg. Chem.* **1984**, *23*, 2336–2343.
- (16) Barigelletti, F.; Flamigni, L.; Balzani, V.; Collin, J.-P.; Sauvage, J.-P.; Sour, A.; Constable, E. C.; Thompson, A. M. W. C. *J. Am. Chem. Soc.* **1994**, *116*, 7692–7699.
- (17) Brewer, R. G.; Jensen, G. E.; Brewer, K. J. *Inorg. Chem.* **1994**, *33*, 124–129.
- (18) Constable, E. C.; Thompson, A. M. W. C. *J. Chem. Soc., Dalton Trans.* **1995**, 1615–1627.
- (19) Demadis, K. D.; El-Samanody, E.-S.; Meyer, T. J.; White, P. S. *Polyhedron* **1999**, *18*, 1587–1594.
- (20) Vogler, L. M.; Brewer, K. J. *Inorg. Chem.* **1996**, *35*, 818–824.
- (21) Clays, K.; Persoons, A. *Rev. Sci. Instrum.* **1992**, *63*, 3285–3289.
- (22) Olbrechts, G.; Strobbe, R.; Clays, K.; Persoons, A. *Rev. Sci. Instrum.* **1998**, *69*, 2233–2241.
- (23) Olbrechts, G.; Wostyn, K.; Clays, K.; Persoons, A. *Opt. Lett.* **1999**, *24*, 403–405.

nm) and $< 3 \times 10^{-5} \text{ M}^{-1}$ (800 and 1300 nm)]; the linearity of the HRS signal as a function of chromophore concentration confirmed that no significant self-absorption of the SHG signal occurred in these experiments.

Ruthenium(II) [5-(4'-Ethylnyl-(2,2';6',2''-terpyridinyl))-10,20-bis(2',6'-bis(3,3-dimethyl-1-butyloxy)phenyl)porphinato]zinc(II)-(2,2';6',2''-terpyridine)²⁺ Bis-hexafluorophosphate ([Ru-PZn-A], 1). [5-Ethylnyl-10,20-bis(2',6'-bis(3,3-dimethyl-1-butyloxy)phenyl)porphinato]zinc(II) (193 mg, 0.20 mmol), ruthenium(II) (4'-bromo-2,2';6',2''-terpyridinyl)(2,2';6',2''-terpyridinyl) bis-hexafluorophosphate (Ru(tpy)₂Br) (200 mg, 0.21 mmol), diisopropylamine (8 mL), THF (30 mL), and acetonitrile (30 mL) were brought together in an oven-dried 100-mL Schlenk tube. The solution was degassed via three freeze-pump-thaw cycles, following which Pd(PPh₃)₄ (50 mg, 0.04 mmol) and CuI (10 mg, 0.05 mmol) were added. The reaction was stirred under N₂ at 70 °C for 24 h, the solution was cooled to room temperature, and the solvent was evaporated. The product was purified by column chromatography on silica using 80:17:3 acetonitrile/water/saturated KNO₃ as the eluant. Compound **1** eluted as a brownish-green band; the volume of the product fraction was reduced to 50 mL, and ammonium hexafluorophosphate (1 g) in 10 mL of water was added, producing a brown precipitate. The product was filtered, washed successively with water and ether, and dried to give 250 mg of compound **1** as the hexafluorophosphate salt (68% yield, based on 193 mg of the [5-ethylnyl-10,20-bis(2',6'-bis(3,3-dimethyl-1-butyloxy)phenyl)porphinato]zinc(II) starting material). ¹H NMR (250 MHz, CD₃CN): 10.15 (s, 1H), 9.99 (d, 2H, *J* = 4.7 Hz), 9.36 (s, 2H), 9.28 (d, 2H, *J* = 4.5 Hz), 9.00 (d, 2H, *J* = 4.6 Hz), 8.82 (d, 2H, *J* = 4.5 Hz), 8.78 (d, 4H, *J* = 8.2 Hz), 8.52 (d, 2H, *J* = 8.0 Hz), 8.45 (t, 1H, *J* = 8.5 Hz), 7.97 (t, 2H, *J* = 8.2 Hz), 7.94 (t, 2H, *J* = 8.2 Hz), 7.81 (t, 2H, *J* = 8.4 Hz), 7.56 (d, 2H, *J* = 5.3 Hz), 7.41 (d, 2H, *J* = 5.3 Hz), 7.2 (m, 4H), 7.17 (d, 4H, *J* = 8.5 Hz), 3.98 (t, 8H, *J* = 7.1 Hz), 0.76 (t, 8H, *J* = 7.0 Hz), 0.19 (s, 36H). LRMS (ESI⁺) *m/z*: 1659.4 (calcd for C₈₈H₈₈N₁₀O₄-Ru₁ZnP₂F₁₂ (M - PF₆)⁺ 1659.5). *m/z*: 757.3 (calcd for C₈₈H₈₈N₁₀O₄-Ru₁Zn (M - 2PF₆)²⁺ 758.8).

Osmium(II) [5-(4'-Ethylnyl-(2,2';6',2''-terpyridinyl))-10,20-bis(2',6'-bis(3,3-dimethyl-1-butyloxy)phenyl)porphinato]zinc(II)-(2,2';6',2''-terpyridine)²⁺ Bis-hexafluorophosphate ([Os-PZn-A], 2). [5-Ethylnyl-10,20-bis(2',6'-bis(3,3-dimethyl-1-butyloxy)phenyl)porphinato]zinc(II) (192 mg, 0.20 mmol), osmium(II) (4'-bromo-2,2';6',2''-terpyridinyl)(2,2';6',2''-terpyridinyl) bis-hexafluorophosphate (Os(tpy)₂Br) (215 mg, 0.21 mmol), diisopropylamine (6 mL), THF (30 mL), and acetonitrile (30 mL) were brought together in an oven-dried 100-mL Schlenk tube. The solution was degassed via three freeze-pump-thaw cycles, following which Pd(PPh₃)₄ (50 mg, 0.04 mmol) and CuI (10 mg, 0.05 mmol) were added. The reaction was stirred under N₂ at 70 °C for 24 h, the solution was cooled to room temperature, and the solvent was evaporated. The product was purified by column chromatography on silica using 80:17:3 acetonitrile/water/saturated KNO₃ as the eluant. The product eluted as a brownish-green band; the volume of the product fraction was reduced to 50 mL, and ammonium hexafluorophosphate (1 g) in 10 mL of water was added, producing a brown precipitate. The product was filtered, washed successively with water and ether, and dried to give 80 mg of compound **2** as the hexafluorophosphate salt (21% yield based on 192 mg of the [5-ethylnyl-10,20-bis(2',6'-bis(3,3-dimethyl-1-butyloxy)phenyl)porphinato]zinc(II) starting material). ¹H NMR (250 MHz, CD₃CN): 10.11 (s, 1H), 10.00 (d, 2H, *J* = 4.6 Hz), 9.38 (s, 2H), 9.27 (d, 2H, *J* = 4.4 Hz), 8.99 (d, 2H, *J* = 4.6 Hz), 8.81 (d, 2H, *J* = 4.3 Hz), 8.75 (m, 4H), 8.48 (d, 2H, *J* = 8.1 Hz), 7.97 (t, 1H, *J* = 8.2 Hz), 7.84 (m, 4H), 7.78 (t, 2H, *J* = 8.4 Hz), 7.75 (m, 4H), 7.41 (d, 2H, *J* = 5.6 Hz), 7.29 (d, 2H, *J* = 5.1 Hz), 7.17 (d, 4H, *J* = 8.5 Hz), 7.12 (4H, m), 3.99 (t, 8H, *J* = 7.1 Hz), 0.78 (t, 8H, *J* = 7.1 Hz), 0.18 (s, 36H). LRMS (ESI⁺) *m/z*: 1604.4 (calcd for C₈₈H₈₈N₁₀O₄OsZn (M - 2PF₆)⁺ 1604.6). *m/z*: 802.2 (calcd for C₈₈H₈₈N₁₀O₄OsZn (M - 2PF₆)²⁺ 802.2).

Ruthenium(II) [5-(4'-Ethylnyl-(2,2';6',2''-terpyridinyl))-15-(4'-nitrophenyl)ethynyl-10,20-bis(2',6'-bis(3,3-dimethyl-1-butyloxy)phenyl)porphinato]zinc(II)-(2,2';6',2''-terpyridine)²⁺ Bis-hexafluorophosphate ([Ru-PZn-A], 3). [5-[(4'-Nitrophenyl)ethynyl]-15-ethylnyl-10,20-bis(2',6'-bis(3,3-dimethyl-1-butyloxy)phenyl)porphinato]zinc(II) (160 mg, 0.15 mmol), Ru(tpy)₂Br (265 mg, 0.28 mmol), diisopropylamine (5 mL), THF (20 mL), and acetonitrile (30 mL) were brought together in an oven-dried 100-mL Schlenk tube. The solution was degassed via three freeze-pump-thaw cycles, following which Pd(PPh₃)₄ (50 mg, 0.04 mmol) and CuI (25 mg, 0.13 mmol) were added. The reaction was stirred under N₂ at 70 °C for 24 h, the solution was cooled to room temperature, and the solvent was evaporated. Compound **3** was purified by column chromatography on silica using 80:17:3 acetonitrile/water/saturated KNO₃ as the eluant. The product eluted as a brownish-green band; the volume of the product fraction was reduced to 50 mL, and ammonium hexafluorophosphate (1 g) in 10 mL of water was added, producing a brown precipitate. The product was filtered, washed successively with water and ether, and dried to give 230 mg of compound **3** as the hexafluorophosphate salt (79% yield, based on 265 mg of the [5-[(4'-nitrophenyl)ethynyl]-15-ethylnyl-10,20-bis(2',6'-bis(3,3-dimethyl-1-butyloxy)phenyl)porphinato]zinc(II) starting material). ¹H NMR (250 MHz, CD₃CN): 9.92 (d, 2H, *J* = 4.5 Hz), 9.37 (s, 2H), 9.30 (d, 2H, *J* = 4.4 Hz), 8.94 (d, 2H, *J* = 4.4 Hz), 8.80 (m, 6H), 8.52 (d, 4H, *J* = 8.1 Hz), 8.45 (t, 1H, *J* = 8.0 Hz), 8.04 (t, 2H, *J* = 7.7 Hz), 7.95 (t, 2H, *J* = 7.8 Hz), 7.86 (t, 2H, *J* = 8.5 Hz), 7.57 (d, 2H, *J* = 5.5 Hz), 7.42 (d, 2H, *J* = 5.5 Hz), 7.24 (m, 8H), 6.91 (d, 2H, *J* = 8.5 Hz), 4.07 (t, 8H, *J* = 7.2 Hz), 0.96 (t, 8H, *J* = 7.2 Hz), 0.30 (s, 36H). MS (MALDI-TOF) *m/z*: 1661 (calcd for C₉₆H₉₁N₁₁O₆RuZn (M - 4PF₆)⁺ 1661) *m/z*: 1807 (calcd for C₉₆H₉₁N₁₁O₆RuZnPF₆ (M - PF₆)⁺ 1806).

Osmium(II) [5-(4'-Ethylnyl-(2,2';6',2''-terpyridinyl))-15-(4'-nitrophenyl)ethynyl-10,20-bis(2',6'-bis(3,3-dimethyl-1-butyloxy)phenyl)porphinato]zinc(II)-(2,2';6',2''-terpyridine)²⁺ Bis-hexafluorophosphate ([Os-PZn-A], 4). [5-[(4'-Nitrophenyl)ethynyl]-15-ethylnyl-10,20-bis(2',6'-bis(3,3-dimethyl-1-butyloxy)phenyl)porphinato]zinc(II) (177 mg, 0.16 mmol), Os(tpy)₂Br (300 mg, 0.29 mmol), diisopropylamine (5 mL), THF (20 mL), and acetonitrile (30 mL) were brought together in an oven-dried 100-mL Schlenk tube. The solution was degassed via three freeze-pump-thaw cycles, following which Pd(PPh₃)₄ (80 mg, 0.07 mmol) and CuI (30 mg, 0.16 mmol) were added. The reaction was stirred under N₂ at 70 °C for 24 h, the solution was cooled to room temperature, and the solvent was evaporated. The product was purified by column chromatography on silica using 80:17:3 acetonitrile/water/saturated KNO₃ as the eluant. The product eluted as a brownish-green band; the volume of the product fraction was reduced to 50 mL, and ammonium hexafluorophosphate (1 g) in 10 mL of water was added, producing a brown precipitate. The product was filtered, washed successively with water and ether, and dried to give 215 mg of compound **4** as the hexafluorophosphate salt (66% yield, based on 177 mg of the [5-[(4'-nitrophenyl)ethynyl]-15-ethylnyl-10,20-bis(2',6'-bis(3,3-dimethyl-1-butyloxy)phenyl)porphinato]zinc(II) starting material). ¹H NMR (250 MHz, CD₃CN): 9.92 (d, 2H, *J* = 4.5 Hz), 9.37 (s, 2H), 9.23 (d, 2H, *J* = 4.4 Hz), 8.94 (d, 2H, *J* = 4.7 Hz), 8.79 (m, 6H), 8.51 (d, 2H, *J* = 8.1 Hz), 7.99 (t, 1H, *J* = 8.2 Hz), 7.84 (m, 6H), 7.44 (d, 2H, *J* = 5.4 Hz), 7.31 (d, 2H, *J* = 5.3 Hz), 7.24 (d, 4H, *J* = 8.5 Hz), 7.13 (m, 6H), 6.69 (d, 2H, *J* = 8.2 Hz), 4.08 (t, 8H, *J* = 7.3 Hz), 0.98 (t, 8H, *J* = 7.2 Hz), 0.32 (s, 36H). MS (MALDI-TOF) *m/z*: 1750 (calcd for C₉₆H₉₁N₁₁O₆OsZn (M - 2PF₆)⁺ 1749).

Ruthenium(II) [5-(4'-Ethylnyl-(2,2';6',2''-terpyridinyl))osmium(II)-15-(4'-ethynyl-(2,2';6',2''-terpyridinyl))-10,20-bis(2',6'-bis(3,3-dimethyl-1-butyloxy)phenyl)porphinato]zinc(II)-bis(2,2';6',2''-terpyridine)⁴⁺ Tetrakis-hexafluorophosphate ([Ru-PZn-Os], 5). Ruthenium(II) [5-(4'-Ethylnyl-(2,2';6',2''-terpyridinyl))-15-ethylnyl-10,20-bis(2',6'-bis(3,3-dimethyl-1-butyloxy)phenyl)porphinato]zinc(II)-(2,2';6',2''-terpyridine)²⁺ bis-hexafluorophosphate (226 mg, 0.12 mmol), Os(tpy)₂Br (363 mg, 0.35 mmol), diisopropylamine (6 mL), THF (30

mL), and acetonitrile (100 mL) were brought together in an oven-dried 350-mL Schlenk tube. The solution was degassed via three freeze-pump-thaw cycles, following which Pd(PPh₃)₄ (60 mg, 0.05 mmol) and CuI (15 mg, 0.08 mmol) were added. The reaction was stirred under N₂ at 70 °C for 24 h, the solution was cooled to room temperature, and the solvent was evaporated. Compound **5** was purified by column chromatography on silica using 80:17:3 acetonitrile/water/saturated KNO₃ as the eluant. Electronic absorption spectroscopy determined that the product eluted after several minor fractions as a brown band. The volume of the product fraction was reduced to 50 mL, and ammonium hexafluorophosphate (1 g) in 10 mL of water was added, giving a brown precipitate. The product was filtered, washed successively with water and ether, and dried to give 76 mg of compound **5** as the hexafluorophosphate salt (23% yield based on 226 mg of the ruthenium(II) 5-[4'-ethynyl-(2,2';6',2''-terpyridinyl)]-15-(ethynyl)bis[10,20-bis(2',6'-bis(3,3-dimethyl-1-butyloxy)phenyl)porphinato]zinc(II)-(2,2';6',2''-terpyridine)²⁺ bis-hexafluorophosphate starting material). ¹H NMR (250 MHz, CD₃CN): 9.98 (d, 2H, *J* = 4.6 Hz), 9.97 (d, 2H, *J* = 4.7 Hz), 9.39 (s, 2H), 9.38 (s, 2H), 8.95 (d, 2H, *J* = 4.5 Hz), 8.94 (d, 2H, *J* = 4.6 Hz), 8.80 (m, 8H), 8.50 (m, 7H), 7.78 (m, 13H), 7.56 (d, 2H, *J* = 5.6 Hz), 7.30 (m, 14H), 4.03 (t, 8H, *J* = 7.0 Hz), 0.85 (t, 8H, *J* = 7.0 Hz), 0.20 (s, 36H). MS (MALDI-TOF) *m/z*: 2483 (calcd for C₁₂₀H₁₀₈N₁₆O₄OsRuZnP₂F₁₂ (M - 2PF₆)⁺ 2483). *m/z*: 2339 (calcd for C₁₂₀H₁₀₈N₁₆O₄OsRuZnP₆ (M - 3PF₆)⁺ 2338). *m/z*: 2194 (calcd for C₁₂₀H₁₀₈N₁₆O₄OsRuZn (M - 4PF₆)⁺ 2194).

[5-(4'-Ethynyl-2,2';6',2''-terpyridyl)-10,20-bis(2',6'-bis(3,3-dimethyl-1-butyloxy)phenyl)porphinato]zinc(II) (6). [5-Ethynyl-10,20-bis(2',6'-bis(3,3-dimethyl-1-butyloxy)phenyl)porphinato]zinc(II) (155 mg, 0.16 mmol), 4'-bromo-2,2';6',2''-terpyridine (280 mg, 0.90 mmol), diisopropylamine (8 mL), and THF (30 mL) were brought together in an oven-dried 100 mL-Schlenk tube. The solution was degassed via three freeze-pump-thaw cycles, following which Pd(PPh₃)₄ (30 mg, 0.026 mmol) and CuI (8 mg, 0.042 mmol) were added. The reaction was stirred under N₂ at 70 °C for 20 h, the solution was cooled to room temperature, and the solvent was evaporated. The product was purified by column chromatography on neutral alumina using 3:2 hexanes/THF as the eluant. The product eluted as a green band; the volatiles were evaporated, and the residual solid was further purified on a size exclusion column (SX-1 biobeads), utilizing a THF eluant. A second round of chromatography on neutral alumina using 1:1 THF/hexanes as the eluant gave 96 mg of pure compound **6** (51% yield based on 155 mg of the [5-ethynyl-10,20-bis(2',6'-bis(3,3-dimethyl-1-butyloxy)phenyl)porphinato]zinc(II) starting material). ¹H NMR (250 MHz, pyridine-*d*₅) 10.14 (s, 1H), 10.08 (d, 2H, *J* = 4.5 Hz), 9.36 (d, 2H, *J* = 4.6 Hz), 9.34 (d, 2H, *J* = 4.5 Hz), 9.31 (s, 2H), 9.36 (d, 2H, *J* = 4.4 Hz), 8.89 (m, 4H), 8.06 (t, 2H, *J* = 8.3 Hz), 7.94 (dt, 2H, *J* = 7.7 Hz, 1.9 Hz), 7.38 (m, 6H), 4.13 (t, 8H, *J* = 7.1 Hz), 0.93 (t, 8H, *J* = 7.5 Hz), 0.33 (s, 36H).

[5,15-Bis(4'-ethynyl-2,2';6',2''-terpyridyl)-10,20-bis(2',6'-bis(3,3-dimethyl-1-butyloxy)phenyl)porphinato]zinc(II) (7). [5,15-Diethynyl-10,20-bis(2',6'-bis(3,3-dimethyl-1-butyloxy)phenyl)porphinato]zinc(II) (123 mg, 0.13 mmol), 4'-bromo-2,2';6',2''-terpyridine (330 mg, 1.06 mmol), diisopropylamine (8 mL), and THF (30 mL) were brought together in an oven-dried 100-mL Schlenk tube. The solution was degassed via three freeze-pump-thaw cycles, following which Pd(PPh₃)₄ (30 mg, 0.026 mmol) and CuI (10 mg, 0.053 mmol) were added. The reaction was stirred under N₂ at 70 °C for 20 h, the solution was cooled to room temperature, and the solvent was evaporated. The product was purified by column chromatography on neutral alumina using 7:3 hexanes/THF as the eluant. The product eluted as a purplish-green band; the volatiles were evaporated, and the residual solid was further purified on a size exclusion column (SX-1 biobeads), utilizing a THF eluant. A second round of chromatography on neutral alumina using 3:2 hexanes/THF as the eluant gave 118 mg of pure compound **7** (63% yield based on 123 mg of the [5,15-diethynyl-10,20-bis(2',6'-bis(3,3-dimethyl-1-butyloxy)phenyl)porphinato]zinc(II) starting mate-

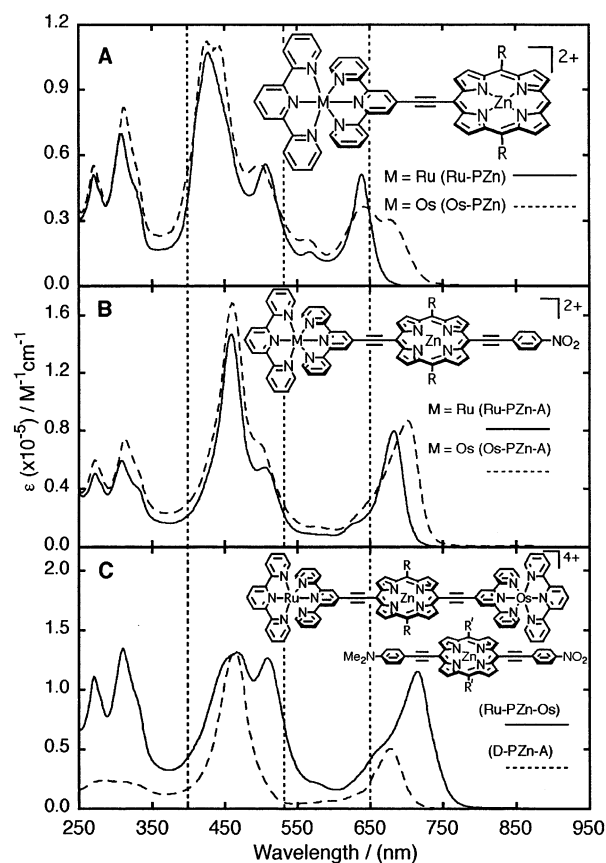


Figure 1. Comparative electronic absorption spectra of (A) Ru-PZn, Os-PZn; (B) Ru-PZn-A, Os-PZn-A; and (C) Ru-PZn-Os, D-PZn-A. Dashed vertical lines indicate the wavelengths corresponding to the respective second harmonics of the fundamental 800, 1064, and 1300 nm incident irradiation. Experimental conditions: *T* = 20 °C; solvent = CH₃CN (Ru/Os-containing compounds), THF (D-PZn-A). R = 2',6'-bis(3,3-dimethyl-1-butyloxy)phenyl, R' = phenyl.

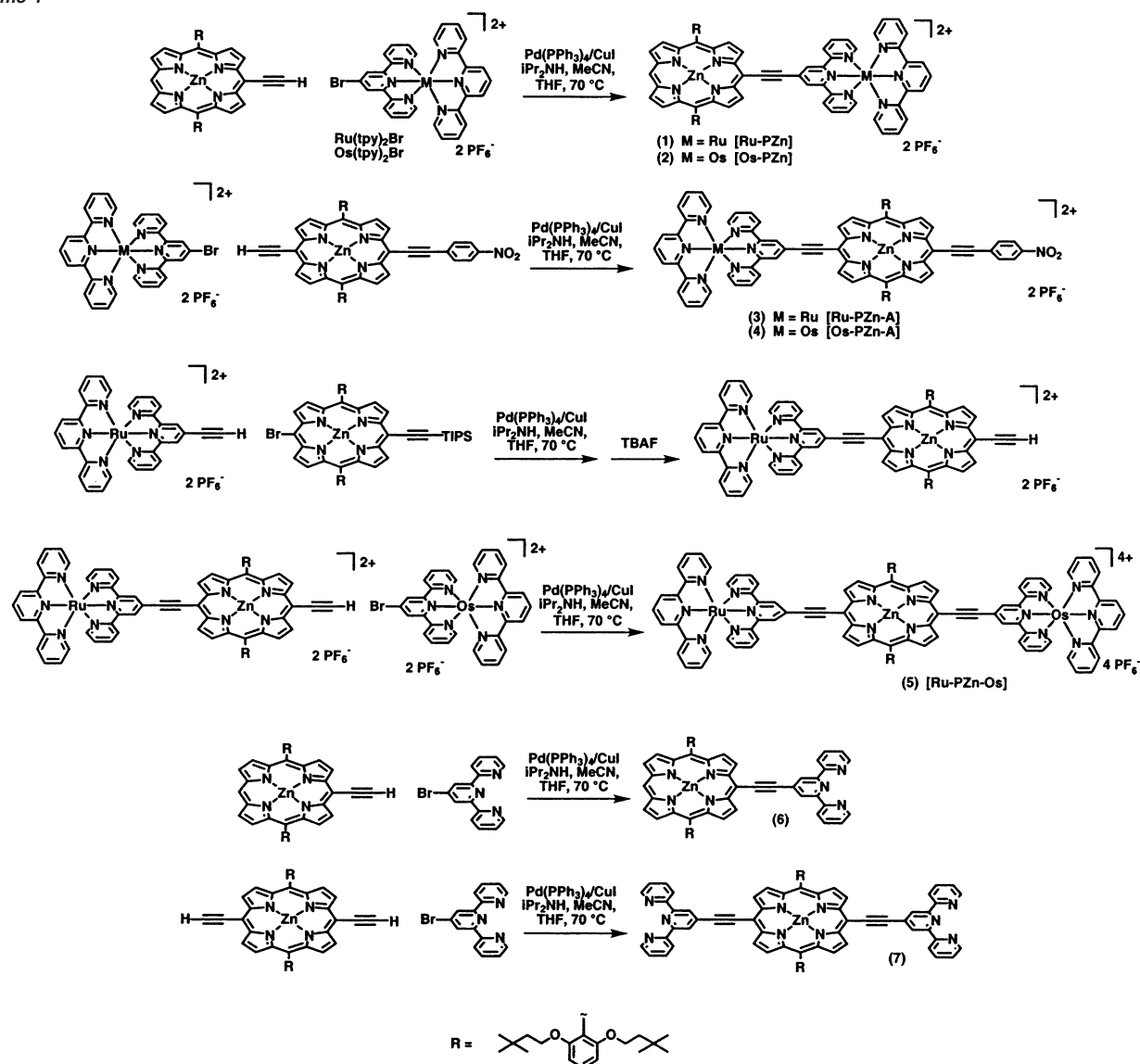
rial). ¹H NMR (250 MHz, pyridine-*d*₅) 10.01 (d, 4H, *J* = 4.5 Hz), 9.30 (s, 4H), 9.25 (d, 4H, *J* = 4.5 Hz), 8.90 (8H, m), 8.08 (t, 2H, *J* = 8.3 Hz), 7.94 (dt, 4H, *J* = 7.7 Hz, 1.9 Hz), 7.40 (8H, m), 4.18 (t, 8H, *J* = 7.5 Hz), 0.99 (t, 8H, *J* = 7.5 Hz), 0.36 (s, 36H).

Results and Discussion

Design. Figure 1 highlights a series of bis- and tris-(chromophoric) supermolecules consisting of (porphinato)zinc(II) [P(Zn)], Ru(tpy)₂, and Os(tpy)₂ units in which an ethynyl moiety bridges the *meso*-macrocycle and 4'-terpyridyl positions. These species were synthesized from porphyrinic and terpyridyl precursor molecules bearing either ethynyl or bromo functional groups via metal-catalyzed cross-coupling reactions.^{6,24–37} Key

- (24) Heck, R. F. *Acc. Chem. Res.* **1979**, *12*, 146–151.
- (25) Takahashi, S.; Kuroyama, Y.; Sonogashira, K.; Hagihara, N. *Synthesis* **1980**, 627–630.
- (26) Kumada, M. *Pure Appl. Chem.* **1980**, *52*, 669–678.
- (27) Negishi, E.-I.; Luo, F. T.; Frisbee, R.; Matsushita, H. *Heterocycles* **1982**, *18*, 117–122.
- (28) Stille, J. K. *Angew. Chem., Int. Ed. Engl.* **1986**, *25*, 508–524.
- (29) Miyaura, N.; Suzuki, A. *Chem. Rev.* **1995**, *95*, 2457–2483.
- (30) DiMaggio, S. G.; Lin, V. S. Y.; Therien, M. J. *J. Am. Chem. Soc.* **1993**, *115*, 2513–2515.
- (31) DiMaggio, S. G.; Lin, V. S. Y.; Therien, M. J. *J. Org. Chem.* **1993**, *58*, 5983–5993.
- (32) Lin, V. S. Y.; Therien, M. J. *Chem.—Eur. J.* **1995**, *1*, 645–651.
- (33) LeCours, S. M.; Guan, H. W.; DiMaggio, S. G.; Wang, C. H.; Therien, M. J. *J. Am. Chem. Soc.* **1996**, *118*, 1497–1503.
- (34) LeCours, S. M.; DiMaggio, S. G.; Therien, M. J. *J. Am. Chem. Soc.* **1996**, *118*, 11854–11864.
- (35) LeCours, S. M.; Phillips, C. M.; de Paula, J. C.; Therien, M. J. *J. Am. Chem. Soc.* **1997**, *119*, 12578–12589.

Scheme 1



design elements of these species exploit the facts that (1) ruthenium polypyridyl compounds possess significant optical³⁸ nonlinearities, outstanding thermal stabilities,^{39–42} and electronically excited states characterized by multidirectional metal-to-ligand charge transfer (MLCT);⁴³ (2) appropriate polypyridyl ethyne derivatization gives rise to a singly degenerate, low-energy electronically excited CT state; and (3) coupling such an ethynylated metal polypyridyl moiety to a PZn *meso*-carbon position enforces a head-to-tail alignment of the corresponding

transition dipoles of the two chromophoric entities,^{6,32–37,44,45} defining a supermolecular structure having an initially prepared singly degenerate excited state polarized along this vector.

Synthesis. The syntheses of these ethyne-bridged (porphyrinato)zinc–bis(terpyridyl)metal compounds are summarized in Scheme 1. The metal-mediated cross-coupling^{6,24–37} of an ethyne-functionalized (porphyrinato)zinc(II) species^{6,30–37} with appropriately halogenated bis(2,2',6',2''-terpyridyl)metal compounds provides entry into this structural class of supermolecular chromophores. These structures contrast conventional covalently linked porphyrin-polypyridyl(metal) assemblies^{46–50} in that a cylindrically π -symmetric bridge directly links the two chromophores.

The Ru-PZn and Os-PZn complexes were prepared by the respective cross-coupling of the 4'-halogenated metal bis(terpyridyl) compounds Ru(tpy)₂Br and Os(tpy)₂Br with 5-ethynyl-10,20-bis(2',6'-bis(3,3-dimethyl-1-butyl)oxy)porphyrinato]-

- (36) Shediach, R.; Gray, M. H. B.; Uyeda, H. T.; Johnson, R. C.; Hupp, J. T.; Angiolillo, P. J.; Therien, M. J. *J. Am. Chem. Soc.* **2000**, *122*, 7017–7033.
 (37) Susumu, K.; Therien, M. J. *J. Am. Chem. Soc.* **2002**, *124*, 8550–8552.
 (38) Vance, F. W.; Hupp, J. T. *J. Am. Chem. Soc.* **1999**, *121*, 4047–4053.
 (39) Dhenaut, C.; Ledoux, I.; Samuel, I. D. W.; Zyss, J.; Bourgault, M.; Lebozec, H. *Nature (London)* **1995**, *374*, 339–342.
 (40) Morrison, I. D.; Denning, R. G.; Laidlaw, W. M.; Stammers, M. A. *Rev. Sci. Instrum.* **1996**, *67*, 1445–1453.
 (41) (a) Warachim, H.; Bujewski, A. *J. Therm. Anal.* **1984**, *29*, 1001–1004.
 (b) Schröder, M.; Stephenson, T. A. *Comprehensive Coordination Chemistry*; Wilkinson, G. F., Gillard, R. D., McCleverty, J. A., Eds.; Pergamon: Oxford, U.K., 1987; Vol. 4, pp 277–522.
 (42) TGA–DTA studies indicate that T_d for Ru-PZn exceeds 325 °C, consistent with literature precedent (see refs 33 and 41).
 (43) Damrauer, N. H.; Cerullo, G.; Yeh, A.; Boussie, T. R.; Shank, C. V.; McCusker, J. K. *Science (Washington D. C.)* **1997**, *275*, 54–57.

- (44) Kumble, R.; Palese, S.; Lin, V. S. Y.; Therien, M. J.; Hochstrasser, R. M. *J. Am. Chem. Soc.* **1998**, *120*, 11489–11498.
 (45) Angiolillo, P. J.; Lin, V. S. Y.; Vanderkooi, J. M.; Therien, M. J. *J. Am. Chem. Soc.* **1995**, *117*, 12514–12527.

Table 1. Electronic Spectral Data for Ru-PZn, Os-PZn, Ru-PZn-A, Os-PZn-A, and Ru-PZn-Os and Chromophoric Benchmarks 6–11

compd	abs band maxima (nm) ($\epsilon \times 10^{-5}$ [M ⁻¹ cm ⁻¹])				³ MLCT	oscillator strength <i>B</i> -band region	oscillator strength <i>Q</i> -band region	total oscillator strength
	<i>B</i> -band	MLCT	<i>Q</i> -state transitions					
Ru-PZn	428 (1.07)	506 (0.56)	567 (0.15)	639 (0.51)		2.10 ^{<i>e,j</i>}	0.27 ^{<i>f</i>}	2.37 ^{<i>g</i>}
Os-PZn	425 (1.12)	498 (0.56)	561 (0.21)	675 (0.30)		2.43 ^{<i>e,j</i>}	0.42 ^{<i>f</i>}	2.85 ^{<i>g</i>}
Ru-PZn-A	440 (1.10)		641 (0.36)					
Ru-PZn-A	459 (1.47)	504 (0.55)	625 (0.16)	682 (0.79)		2.04 ^{<i>e,j</i>}	0.41 ^{<i>f</i>}	2.45 ^{<i>g</i>}
Os-PZn-A	459 (1.68)	499 (0.71)	573 (0.14)	702 (0.87)		2.53 ^{<i>e,j</i>}	0.62 ^{<i>f</i>}	3.15 ^{<i>g</i>}
Ru-PZn-Os	456 (1.28)	509 (1.27)	573 (0.22)	715 (1.16)		3.38 ^{<i>h,j</i>}	0.79 ^{<i>i</i>}	4.17 ^{<i>g</i>}
6	441 (3.86)		567 (0.16)	618 (0.26)		1.89 ^{<i>e</i>}	0.17 ^{<i>f</i>}	2.06 ^{<i>g</i>}
7	454 (4.88)			659 (0.66)		2.04 ^{<i>e</i>}	0.30 ^{<i>f</i>}	2.34 ^{<i>g</i>}
8	430 (2.92)		563 (0.12)	606 (0.07)		1.39 ^{<i>a</i>}	0.08 ^{<i>b</i>}	1.47 ^{<i>c</i>}
9	438 (3.82)		580 (0.12)	634 (0.29)		2.34 ^{<i>a</i>}	0.16 ^{<i>b</i>}	2.50 ^{<i>c</i>}
10		483 (0.20)						0.31 ^{<i>d</i>}
11		482 (0.16)			665 (0.04)			0.24 ^{<i>d</i>}

^a Oscillator strengths calculated over the 290 → 480 wavelength domain. ^b Oscillator strengths calculated over the 480 → 850 wavelength domain. ^c Oscillator strengths calculated over the 290 → 850 wavelength domain. ^d Oscillator strengths calculated over the 380 → 850 wavelength domain. ^e Oscillator strengths calculated over the 360 → 555 wavelength domain. ^f Oscillator strengths calculated over the 555 → 850 wavelength domain. ^g Oscillator strengths calculated over the 360 → 850 wavelength domain. ^h Oscillator strengths calculated over the 360 → 600 wavelength domain. ⁱ Oscillator strengths calculated over the 600 → 850 wavelength domain. ^j Includes contributions from metal polypyridyl-derived transitions.

zinc(II) (Scheme 1). Ru-PZn-A and Os-PZn-A were prepared in a similar fashion, utilizing a PZn intermediate featuring 5-ethynyl and 15-(nitrophenyl)ethynyl substituents (Scheme 1). Ru-PZn-Os was prepared in a stepwise manner in which a 4'-ethynyl ruthenium bis(terpyridyl) compound was cross-coupled to a PZn complex functionalized with 5-triisopropylsilylethynyl and 15-bromo substituents. Removal of the triisopropylsilyl protecting group followed by a second cross-coupling with osmium(II) (4'-bromo-2,2';6',2''-terpyridinyl)(2,2';6',2''-terpyridinyl)-bis-hexafluorophosphate, gave the desired complex (Scheme 1).

Compounds Ru-PZn, Os-PZn, Ru-PZn-A, Os-PZn-A, and Ru-PZn-Os were isolated via column chromatography on silica using CH₃CN/H₂O/saturated KNO₃ as the eluant. Purification of key precursor compounds [5-(4'-ethynyl-2,2';6',2''-terpyridyl)-10,20-bis(2',6'-bis(3,3-dimethyl-1-butylloxy)phenyl)porphinato]zinc(II) (**6**) and [5,15-bis(4'-ethynyl-2,2';6',2''-terpyridyl)-10,20-bis(2',6'-bis(3,3-dimethyl-1-butylloxy)phenyl)porphinato]zinc(II) (**7**) (Scheme 1) utilized neutral alumina as the chromatographic stationary phase. Ru-PZn, Os-PZn, Ru-PZn-A, Os-PZn-A, and Ru-PZn-Os were isolated as their hexafluorophosphate salts via metathesis reactions.

Electronic Absorption Spectroscopy. Consistent with the design features of Ru-PZn, Os-PZn, Ru-PZn-A, Os-PZn-A, and Ru-PZn-Os noted above, the electronic spectra of these species (Figure 1) evince strong mixing of PZn-based oscillator strength

with metal polypyridyl charge–resonance bands and display a variety of new low energy electronic transitions that feature significant μ_{ge}^2 values and large extinction coefficients. Two aspects of these electronic spectra (Figure 1) are particularly noteworthy: (i) they differ markedly from those characteristic of monomeric ethyne-elaborated PZn and Ru(tpy)₂ chromophores (Supporting Information),^{6,32–36,51,52} and (ii) they display an unusual degree of spectral coverage of the 250–750 nm energy domain. In this latter regard, note that the extinction coefficient of Ru-PZn-Os's absorption *minimum* over this wavelength range (at ~ 610 nm) exceeds 15 000 M⁻¹ cm⁻¹. Table 1 lists the spectral data for these compounds, along with that obtained for key functionalized chromophoric precursor molecules **6**, **7**, [5-triisopropylsilylethynyl-10,20-bis(2',6'-bis(3,3-dimethyl-1-butylloxy)phenyl)porphinato]zinc(II) (**8**), [5,15-bis-trimethylsilylethynyl-10,20-di(2',6'-bis(3,3-dimethyl-1-butylloxy)phenyl)porphinato]zinc(II) (**9**), [Ru(tpy)(4'-trimethylsilylethynyl-tpy)](PF₆)₂ (**10**), and [Os(tpy)(4'-trimethylsilylethynyl-tpy)](PF₆)₂ (**11**); optical spectra of these chromophoric benchmarks are contained within the Supporting Information.

The optical spectra of compounds **6** and **7** contrast with those obtained for Ru-PZn, Os-PZn, Ru-PZn-A, Os-PZn-A, and Ru-PZn-Os; note that the electronic absorption spectra of *meso*-ethynyl-terpyridine functionalized PZn compounds **6** and **7** (Supporting Information) resemble those reported previously for 5- and [5,15-di(arylethynyl)porphinato]zinc(II) complexes,^{33–35,53} indicating that the building block Ru/Os- and ligand-derived electronic transitions figure prominently in the coupled oscil-

(46) Harriman, A.; Odobel, F.; Sauvage, J. P. *J. Am. Chem. Soc.* **1994**, *116*, 5481–5482.

(47) Collin, J.-P.; Harriman, A.; Heitz, V.; Odobel, F.; Sauvage, J.-P. *J. Am. Chem. Soc.* **1994**, *116*, 5679–5690.

(48) Harriman, A.; Odobel, F.; Sauvage, J.-P. *J. Am. Chem. Soc.* **1995**, *117*, 9461–9472.

(49) Flamigni, L.; Barigelletti, F.; Armaroli, N.; Ventura, B.; Collin, J. P.; Sauvage, J. P.; Williams, J. A. G. *Inorg. Chem.* **1999**, *38*, 661–667.

(50) Dixon, I. M.; Collin, J.-P.; Sauvage, J.-P.; Barigelletti, F.; Flamigni, L. *Angew. Chem., Int. Ed.* **2000**, *39*, 1292–1295.

(51) Sauvage, J. P.; Collin, J. P.; Chambron, J. C.; Guillerez, S.; Coudret, C.; Balzani, V.; Barigelletti, F.; De Cola, L.; Flamigni, L. *Chem. Rev.* **1994**, *94*, 993–1019.

(52) Gouterman, M. *J. Mol. Spectrosc.* **1961**, *6*, 138–163.

(53) Karki, L.; Vance, F. W.; Hupp, J. T.; LeCours, S. M.; Therien, M. J. *J. Am. Chem. Soc.* **1998**, *120*, 2606–2611.

Table 2. Dynamic Hyperpolarizabilities [β_λ Values, ($\times 10^{-30}$ esu)] Determined via HyperRayleigh Light Scattering Experiments^a

compd	β_{800}^b	β_{1064}	β_{1300}
Ru-PZn	<50 ^c	2100	5100
Os-PZn	<50 ^c	2600	<50 ^c
Ru-PZn-A	220	4000	2400
Os-PZn-A	250	5000	<50 ^c
Ru-PZn-Os	240	4500	860
D-PZn-A	5142 ^d	4933 ^d	<i>e</i>

^a Conditions: $T = 20$ °C, solvent = CH_2Cl_2 . β_λ values reported are independent of the frequency modulation of the fundamental beam (DC to 960 MHz; see exemplary data in Figure 2), indicating that multiphoton fluorescence contributions to the observed HRS signals are absent. See refs 22, 23, 54, 55, and 64. ^b Dynamic hyperpolarizabilities determined at $\lambda_{\text{inc}} = 800$ nm for Ru-PZn, Os-PZn, Ru-PZn-A, Os-PZn-A, and Ru-PZn-Os and at $\lambda_{\text{inc}} = 830$ nm for D-PZn-A. ^c Upper limit corresponds to the smallest HRS signal that can be measured accurately. ^d See ref 33. ^e Not measured.

lator photophysics manifest by the Ru-PZn, Os-PZn, Ru-PZn-A, Os-PZn-A, and Ru-PZn-Os supermolecules.

Nonlinear Optical Properties. Table 2 lists β_λ values for Ru-PZn, Os-PZn, Ru-PZn-A, Os-PZn-A, and Ru-PZn-Os determined from hyperRayleigh light scattering (HRS) measurements^{22,54,55} and highlights the frequency dependence of the NLO response observed for fundamental incident irradiation wavelengths (λ_{inc}) of 800, 1064, and 1300 nm. Tabulated here as well are analogous HRS data obtained for the benchmark PZn-based NLO chromophore 5-(4'-dimethylaminophenylethynyl)-15-(4''-nitrophenylethynyl)-10,20-diphenylporphinato]zinc(II) (D-PZn-A) (Figure 1C), a high $\mu\beta_0$ pigment which possesses β_{830} and β_{1064} values near 5000×10^{-30} esu, a β_{1906} value of 1000×10^{-30} esu, and a static hyperpolarizability (β_0) of $\sim 800 \times 10^{-30}$ esu.^{33,53,56}

The trends observed in Table 2 are unusual. For example, the HRS data show that while for Ru-PZn, the absolute magnitude of the dynamic hyperpolarizability ($|\beta_\lambda|$) increases with increasing λ_{inc} (800 \rightarrow 1064 \rightarrow 1300 nm), structurally related Os-PZn displays a $|\beta_\lambda|$ maximum at 1064 nm and β_λ s $< 50 \times 10^{-30}$ esu at 800 and 1300 nm. Ru-PZn-A and Ru-PZn-Os express modest β_λ values for incident irradiation at 800 nm, large β_λ s at 1064 nm, and β_λ s of 2400 and 860×10^{-30} esu, respectively, at 1300 nm. The λ_{inc} -dependent trend in β_λ values for Os-PZn-A resembles that observed for Os-PZn, with the large observed β_{1064} value diminishing to approximately zero at $\lambda_{\text{inc}} = 1300$ nm.

The λ_{inc} -dependent trend in β_λ values for D-PZn-A is well understood.^{33,53,56} It derives from the expected resonance enhancement effects and the facts that both the x -polarized porphyrin B and Q states possess identical CT character and β_0 s of the same sign; β_λ contributions from the B - and Q -derived transitions thus have opposite signs when two-photon resonance frequencies lie between the B - and Q -derived transitions (e.g., when $\lambda_{\text{inc}} = 1064$ nm). Similar nonlinear optical behavior has been noted in (dicyanomethylene)pyran chromophores, in which two low lying CT transitions contribute to the static hyperpolarizability.⁵⁷ While NLO response frequency dispersion effects driven by the presence of multiple CT transitions undoubtedly play a role in determining the magnitudes of β_λ listed in Table

(54) Terhune, R. W.; Maker, P. D.; Savage, C. M. *Phys. Rev. Lett.* **1965**, *14*, 681–684.

(55) Clays, K.; Persoons, A. *Phys. Rev. Lett.* **1991**, *66*, 2980–2983.

(56) Priyadarshy, S.; Therien, M. J.; Beratan, D. N. *J. Am. Chem. Soc.* **1996**, *118*, 1504–1510.

Table 3. Oxidative and Reductive Cyclic Voltammetric Data^a for Ru-PZn, Os-PZn, Ru-PZn-A, Os-PZn-A, and Ru-PZn-Os and Potentiometric Benchmarks **8–11**

compd	potentiometric data (mV)					
	ZnP/ZnP ⁺	ZnP ⁺ /ZnP ²⁺	M ²⁺ /M ³⁺	tpy ⁻ /tpy ⁰	ZnP ⁻ /ZnP ⁰	tpy ²⁻ /tpy ⁻
Ru-PZn	870	1130	1465	-1065	-1365	-1575
Os-PZn	845	1075 ^b	1075 ^b	-1040	-1340	-1575
Ru-PZn-A	910	1150	1430	-990	-1260	
Os-PZn-A	900	1210	1090	-990	-1230	
Ru-PZn-Os ^c						
8	765	965			-1420	
9	820	1300			-1230	
10			1275	-1145		-1445
11			950	-1115		-1420
						-1840 ^b

^a Experimental conditions: [chromophore] = 1–3 mM; scan rate = 0.5 V/s; reference electrode = Ag wire. $E_{1/2}$ values reported are relative to SCE; the ferrocene/ferrocenium couple (0.43 V vs SCE) was used as the internal standard. Potentiometric data for compounds **8–11** were obtained in 0.1 M TBABF₄/dimethylformamide, while that for Ru-PZn, Os-PZn, Ru-PZn-A, Os-PZn-A, and Ru-PZn-Os utilized a 0.1 M TBAPF₆/dichloromethane electrolyte/solvent system. The experimental uncertainty in these reported potentials is ± 10 mV. All reported values correspond to one electron redox couples unless noted otherwise. ^b The Os^{II}/Os^{III} and the ZnP⁺/ZnP²⁺ redox couples appear to be coincident or near coincident. ^c Compound Ru-PZn-Os exhibited complex and irreversible redox behavior in the solvent/electrolyte systems listed above.

2, the nature of the extensive mixing of B, Q, and CT electronic states evinced for Ru-PZn, Os-PZn, Ru-PZn-A, Os-PZn-A, and Ru-PZn-Os in Figure 1 is considerably more complex relative to that manifested in D-PZn-A: this derives from the fact that these species possess at least three redox active components (metal, tpy, and PZn). Potentiometric data for these compounds are listed in Table 3.

The oxidative and reductive electrochemical data indicate that at least for Ru-PZn, Os-PZn, Ru-PZn-A, and Os-PZn-A, the observed anodic and cathodic potentiometric responses trace their genesis to established metal polypyridyl- and PZn-redox processes, indicating that the singly, doubly, and triply oxidized- and reduced-ground states of these species correspond to cation and anion states that are largely localized on the building block chromophores (Table 3). These potentiometric data permit a preliminary analysis of the observed frequency dispersion effects in the NLO response of these species.

A qualitative analysis of the nature of the x -polarized transitions in Ru-PZn and Os-PZn, based on potentiometric data and the Gibbs free energy relation, suggests that B - and Q -state $\Delta\mu_{\text{ge}}$ values have opposite signs: M(tpy)₂-to-PZn charge resonance is thermodynamically favored with B -state excitation, while PZn-to-M(tpy)₂ CT occurs with excitation of the x -polarized Q state.⁵⁸ Because B - and Q -state β_0 s would thus have opposite signs when the expected resonance enhancements effects predicted in a classic 2-level formulation of β (eq 1)^{59–61}

(57) Moylan, C. R.; Ermer, S.; Lovejoy, S. M.; McComb, I. H.; Leung, D. S.; Wortmann, R.; Krdmer, P.; Twieg, R. J. *J. Am. Chem. Soc.* **1996**, *118*, 12950–12955.

(58) $-(\Delta G_{\text{CS}}) = E_{(0,0)} - E_{1/2}(D/D^+) + E_{1/2}(A^-/A)$, where $E_{(0,0)}$ is the two-photon resonance energy and the $E_{1/2}(D/D^+)$ and $E_{1/2}(A^-/A)$ values were determined from cyclic voltammetric data (see Table 3). Ru-PZn: Ru^{2+/3+} = 1.47 V, PZn⁻⁰ = -1.37 V, Ru(tpy)⁻⁰ = -1.07 V, PZn^{0/+} = 0.87 V. Os-PZn: Os^{2+/3+} = 1.08 V, PZn⁻⁰ = -1.34 V, Os(tpy)⁻⁰ = -1.04 V, PZn^{0/+} = 0.85 V. The nature of the $E_{(0,0)}$ -dependent CT transition was estimated by approximating $-(\Delta G_{\text{CS}})$ for all possible charge separations and determining which was the most thermodynamically favorable under the assumption that one full unit of charge migrates at these resonance energies. A similar analysis can be used to rationalize the λ_{inc} -dependent HRS data for Ru-PZn-A, Os-PZn-A, and Ru-PZn-Os.

$$\beta'_n = \frac{6(P_{ge})_n^2(\Delta\mu_{ge})_n(E_{op})_n^2}{[(E_{op})_n^2 - (2E_{inc})^2][(E_{op})_n^2 - E_{inc}^2]} \quad (1)$$

(where E_{op} is the energy of the optical transition of interest) are considered, B - and Q -state derived contributions to β_λ will have the same sign when the two-photon resonance frequencies lie between the B - and Q -derived transitions and will have opposite signs at both short and long wavelength, resulting in a cancellation of the HRS signal when $\lambda_{inc} = 800$ and 1300 nm. For both the Ru-PZn and Os-PZn cases, this cancellation is effectively complete when $\lambda_{inc} = 800$ nm. Note that the optical spectra of Figure 1 along with eq 1 predict qualitatively that Ru-PZn's Q -state derived contributions to β_λ at 1300 nm will be large and positive, with the corresponding B -state derived contribution being small and negative, giving a large net β_{1300} value. In contrast, while Os-PZn's B -state derived contribution to β_{1300} is also small and negative, note that its Q -state derived β_λ contribution will be small and positive, as near-equivalent amounts of x -polarized Q -state oscillator strength are distributed to the blue and the red of the 2-photon absorption at 650 nm (Figure 1), resulting in effective canceling of the HRS signal when $\lambda_{inc} = 1300$ nm. Presumably, for the Os-PZn and Os-PZn-A systems that exhibit highly diminished HRS signals at 1300 nm, because the energy denominator (eq 1) increasingly favors contributions from the lowest energy excited state in a two-level formulation of the first-order hyperpolarizability as the zero frequency limit is approached,^{59,62} these species would be predicted to manifest modest, finite β_λ s for longer λ_{inc} , given the nature and extensive oscillator strength of their respective Q -derived transitions. Because of the complex electronic structure of the Ru-PZn, Os-PZn, Ru-PZn-A, and Os-PZn-A compounds, a fully quantitative analysis of the frequency dispersion effects manifest in the NLO responses of these species will require further spectroscopic experiments, the syntheses of related derivatives, and substantive theoretical studies; nonetheless, the hypothesis based on potentiometric data that B - and Q -state contributions to the static hyperpolarizability have opposite signs in these supermolecular chromophores qualitatively accounts for the general trends manifest in the λ_{inc} -dependent magnitudes of $|\beta_\lambda|$ chronicled in Table 2.

Finally, it is important to emphasize that the large β_λ values listed in Table 2 do not derive in part from multiphoton fluorescence contributions to the hyperRayleigh scattering signal. First, it is known that Ru-PZn, Os-PZn, Ru-PZn-A, Os-PZn-A, and Ru-PZn-Os are all nonemissive at ambient temperature.⁶³ For further experimental proof that multiphoton fluorescence contributions to the HRS signal are indeed absent, HRS experiments were performed as a function of amplitude modulation frequency up to 1 GHz.^{22,23,54,55,64} Because of the fact that fluorescence lifetimes are finite, any fluorescence contribution would be demodulated at such frequencies and evident experimentally as an HRS signal that decreased with increasing modulation frequency. Figure 2 shows such exemplary data

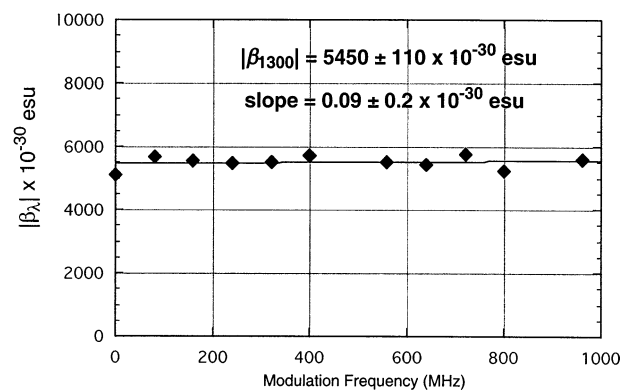


Figure 2. Measured β_{1300} Values for Ru-PZn Determined as a Function of Modulation Frequency.

obtained for RuPZn; note that the measured HRS signal is constant up to 1 GHz, showing conclusively that the large β_{1300} value of 5100×10^{-30} esu (Table 2) is not overestimated because of multiphoton fluorescence.

Conclusions

In summary, this work highlights that: (i) Coupled oscillator photophysics⁶⁵ and metal-mediated cross-coupling can be exploited to elaborate high β_0 supermolecules. (ii) High-stability metal polypyridyl compounds constitute an attractive alternative to electron releasing dialkyl- and diaryl-amino groups, the most commonly used donor moieties in a wide range of established NLO dyes and long recognized to be the moiety that often limits dye thermal stability.^{41–42,66} (iii) Given the NLO response highlighted by Ru-PZn and the fact that its β_λ value determined at 1300 nm exceeds by a factor of 2.5 that determined for any other chromophore at this energy,⁶⁷ this design strategy clearly enables ready elaboration of *extraordinarily large* β_λ chromophores at telecommunication-relevant wavelengths. (iv) An important new effect has been delineated in this series of compounds, namely that B - and Q -state-derived β_0 values can be designed to have the same or opposite sign; because the sign of the resonance enhancement factor is frequency dependent, appropriate engineering of the relative contributions of these CT states at a given wavelength provides a new means to regulate the magnitude of dynamic hyperpolarizabilities and, thus, may enable the development of novel materials with enhanced and more selective electrooptic and NLO properties.

Acknowledgment. This work was supported by a grant from the Office of Naval Research N00014-01-1-0725, the Belgian Government (IUAP/5/3), the Flemish Fund for Scientific Research (G.0261.02), and the University of Leuven (GOA/2000/03).

Supporting Information Available: Syntheses and characterization data for precursor compounds, along with benchmark optical spectra for the ethyne-elaborated bis(terpyridyl)metal and (porphinato)zinc(II) building blocks. This material is available free of charge via the Internet at <http://pubs.acs.org>.

JA020651Q

(59) Oudar, J. L.; Chemla, D. S. *J. Chem. Phys.* **1977**, *66*, 2664–2668.

(60) Oudar, J. L. *J. Chem. Phys.* **1977**, *67*, 446–457.

(61) Willetts, A.; Rice, J. E.; Burland, D. M.; Shelton, D. P. *J. Chem. Phys.* **1992**, *97*, 7590–7599.

(62) Ward, J. F. *Rev. Mod. Phys.* **1965**, *37*, 1–8.

(63) Duncan, T. V.; Rubtsov, I. V.; Miloradovic, I. R.; Uyeda, H. T.; Troxler, T.; Therien, M. J. Manuscript in preparation.

(64) Olbrechts, G.; Clays, K.; Wostyn, K.; Persoons, A. *Synth. Met.* **2000**, *115*, 207–211.

(65) Toury, T.; Zyss, J.; Cherynak, V.; Mukamel, S. *J. Phys. Chem. A* **2001**, *105*, 5692–5703.

(66) Moylan, C. R.; Twieg, R. J.; Lee, V. Y.; Swanson, S. A.; Betterton, K. M.; Miller, R. D. *J. Am. Chem. Soc.* **1993**, *115*, 12599–12600.

(67) Clays, K.; Wostyn, K.; Olbrechts, G.; Persoons, A.; Watanabe, A.; Nogi, K.; Duan, X.-M. *J. Opt. Soc. Am. B* **2000**, *17*, 256–265.